Journal of Materials Chemistry C

Accepted Manuscript

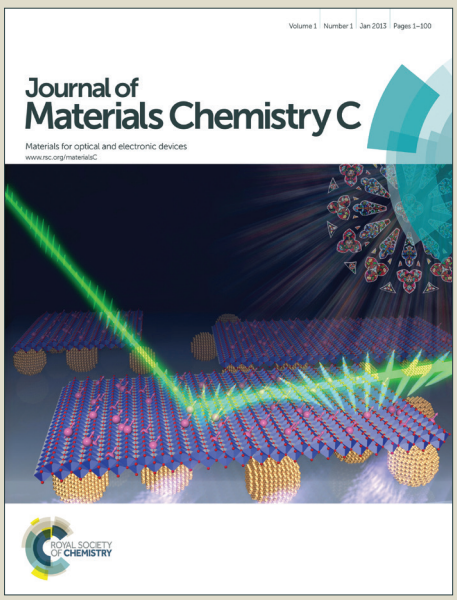

ROYAL SOCIETY OF CHEMISTRY

www.rsc.org/materialsC

Journal of Materials Chemistry C RSCPublishing

COMMUNICATION

Bio-Inspired Iridescent Layer-by-Layer-Assembled Cellulose Nanocrystal Bragg Stacks†

Cite this: DOI: 10.1039/xoxxoooooox

P. Tzeng[a], D.J. Hewson[b], P. Vukusic[b], S.J. Eichhorn[b*], J.C. Grunlan[c*]

Received ooth January 2012,
Accepted ooth January 2012

DOI: 10.1039/xoxxoooooox

www.rsc.org/

Layer-by-layer (LbL) assembly was used to fabricate a synthetic analogue of the color producing multilayered structure commonly found in many biological systems, particularly Coleoptera. The resulting iridescent films comprise multiple LbL-deposited layers designed to control color appearance through the materials' refractive indices and individual multilayer layer thicknesses. The fabricated systems, referred to as Bragg stacks, exhibited very similar optical behavior to the model and the beetle, selectively reflecting the desired color in a narrow band of visible wavelengths and displaying iridescent behavior.

Introduction

The iridescent colors observed in biological systems are notable for their variety and brilliance. The mechanisms that give rise to these colors are of interest to researchers representing a wide variety of primary fields.[1-3] Many examples of iridescent color are found in Coleoptera. The optically brilliant appearance of many beetles is derived from photonic structures found in the species integument.[4, 5] The simplest form of photonic structure associated with the beetle cuticle comprises very thin layers of two materials possessing contrasting refractive indices (RI). Constructive interference of reflected light, or Bragg reflection, can be achieved by such systems when the optical thickness of each periodic layer is on the order of $\lambda/4$ and the viewing angle is close to 90°.[6, 7] Successful, affordable fabrication of such structures could make Bragg reflectors useful for sensing,[8, 9] optical filters,[10, 11] and the widespread replacement of pigment-based coatings.[12, 13] The iridescent effect can only be generated by structural systems and is particularly conspicuous to the human eye, which is appealing to industries where aesthetics are important. The complexity of these structures makes them useful for security, where marks of authentication are required.

Commonly used methods to deposit Bragg stacks include chemical vapor deposition (CVD)[14, 15] and physical vapor deposition (PVD).[16, 17] These techniques are size-limited and have lots of process complexity. Another approach is the use of sol-gel processing via spin coating, dip coating or casting. Despite its simple process and variety of choice in materials, sol-gel techniques suffer from issues of poor uniformity and cracking (heat treatment required for improvement) over larger areas.[18, 19] In order to create a periodic structure with high uniformity, layer-by-layer (LbL) deposition was applied by assembling oppositely charged materials from water. The variety of materials that are available and the simple process (i.e., aqueous solutions under ambient conditions) makes LbL assembly a useful method to fabricate Bragg reflectors. Rubner et al. were the first to demonstrate the ability to generate structural color using LbL deposition.[10, 20] Over the past two decades, the LbL assembly technique has received significant attention due to the manner in which precise control of thin film structure is possible through adjustment of solution concentration,[21, 22] pH/ionic strength,[23, 24] temperature,[25, 26] molecular weight[27, 28] and deposition time[29, 30] of the aqueous deposition mixtures. The multifunctionality of LbL assemblies enable its application in drug delivery,[31, 32] gas barrier/separation,[33, 34] biosensing,[35, 36] wettability control[37, 38] and flame retardancy.[39, 40] Most importantly, this simple deposition process makes industrialization possible, with the potential for scaling up to a continuous dipping[41] or even a continuous spraying process.[42]

In this study, layer-by-layer deposition was used to fabricate uniform Bragg stack optical reflecting systems, similar in form and behavior to the layered structure responsible for the color appearance of the *Chrysochroa. rajah* beetle. Mimicking such beetle cuticle so closely suggests that this simple, aqueous and environmentally-benign methodology could be used to mimic other natural structures (e.g., mother of pearl). The refractive

[a] Department of Chemical Engineering, Texas A&M University, 3122 TAMU, College Station, Texas 77843-3122, United States.
[b] College of Engineering, Maths & Physical Sciences, University of Exeter, Exeter, Devon, EX4 4QL, UK. E-mail: s.j.eichhorn@exeter.ac.uk
[c] Department of Mechanical Engineering, Department of Materials Science & Engineering, Department of Chemistry, Texas A&M University, 3123 TAMU, College Station, Texas 77843-3123, United States. E-mail: jgrunlan@tamu.edu
† Electronic Supplementary Information (ESI) available: Experimental details. See DOI: XXXXXXXX.

index (RI) of each assembled layer was controlled by combining two materials in appropriate proportions in each layer. Thickness was controlled by varying the number of cation/anion deposition cycles, known as "bilayers" (BL), within each layer. The high RI layer (layer A) comprised 13 bilayers of cationic polyethylenimine (PEI) and anionic vermiculite clay (VMT), as shown in Fig. 1a. Electrostatic bonding between PEI and the face of VMT platelets, forces the high aspect ratio disks to deposit parallel to the substrate, forming a dense layer. The low RI layer (layer B) comprised 40 BL of cationic colloidal silica (SiO_2) and anionic cellulose nanocrystals (CNCs). CNCs were selected because they are renewable, have an intrinsic anionic surface charge and high aspect ratio (~18). These features produce highly porous assemblies with colloidal silica to create a low refractive index. While CNCs have been successfully used in LbL assembly to produce anti-reflective films,[43] this study demonstrates their first use with LbL assembly to produce iridescent, biomimetic, Bragg reflectors.

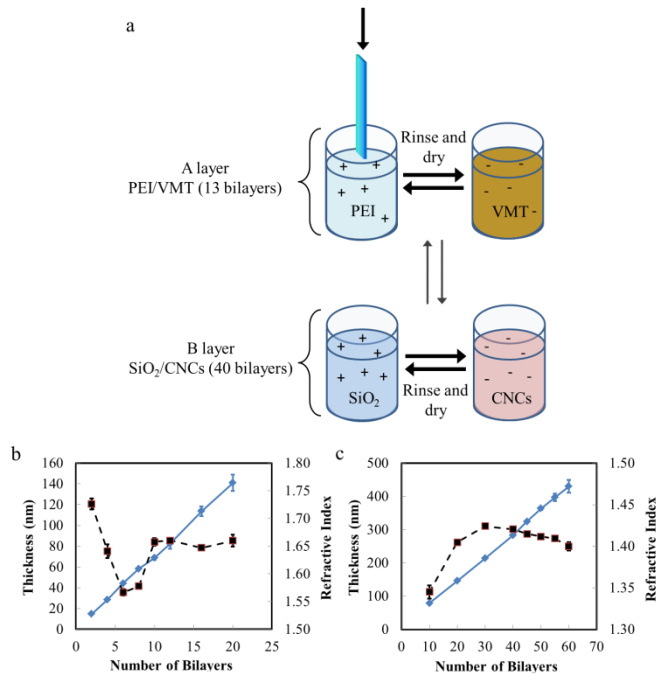

Fig. 1 (a) Schematic of the Bragg stack LbL assembly process. Thickness and refractive index of (b) PEI/VMT and (c) SiO_2/CNCs combinations as a function of bilayers deposited. Error bars indicate standard deviations from the mean.

Results and Discussion

The growth profiles shown in Fig. 1b and 1c show the evolution of film thickness and refractive index as a function of the number of bilayers deposited in the stack. This information is given for both PEI/VMT and SiO_2/CNCs, respectively. Both systems exhibit linear growth, which is typical for bilayers containing nanoparticles.[10, 20, 22] The relationship between the number of bilayers and RI was not linear and evolves differently in each case. The RI in PEI/VMT shows greater consistency after 10 bilayers, where it ranges from 1.65-1.66. SiO_2/CNCs show a gradual decrease in RI with increasing bilayers before leveling out from 20 to 60 bilayers, ranging from 1.40-1.42. It is in these bilayer ranges (above 10 for PEI/VMT and above 20 for SiO_2/CNCs) where consistent Bragg stripes can be deposited.

Modelling of various thickness and RI values taken from the growth profiles revealed a combination for a stack that would lead to bright reflectance in the green region of the visible spectrum. The thicknesses and RIs for the A and B layers (see fig. 1) were 91.4 and 288 nm, and 1.7 and 1.40, respectively. The structures of the stacks were characterized using SEM and TEM and compared to the layered system in the integument of a *C. rajah* beetle. Fig. 2a shows a TEM image of the cross-section through a structurally colored elytron of a *C. rajah* beetle. The periodicity visible in Fig. 2a is derived from the alternating light contrasted and dark contrasted layers aligned parallel to the elytral surface. This differential contrast is associated with differential uptake of the staining chemicals in the elytron during TEM sample preparation. In the beetle itself, the high RI is understood to arise from regions rich in melanin compared to the regions low in melanin content that are associated with low RI. The TEM images of cross sections of the fabricated set of films, comprising alternating light contrasted and dark contrasted layers, is shown in Fig. 2c and 2d. Upon closer inspection of the A layer (Fig. 2d), a distinguishable laminar arrangement of VMT (the darker lines) and PEI can be discerned. The curvature in the layers is understood to be a result of the microtoming process where sample sectioning and exposure to water may compromise the structural integrity of the film. Fig. 2b is a SEM image of a cross-section of an $(AB)_{24}A$ film, providing information about the B layer structure not discernable in the TEM images. It confirms the dense laminar structure of the A layers. The colloidal silica and the CNCs have formed an isotropic porous structure. This was one of the intentions of the fabrication process because such porosity helps to generate a low RI due to an averaging of the RIs of the solid material and air.

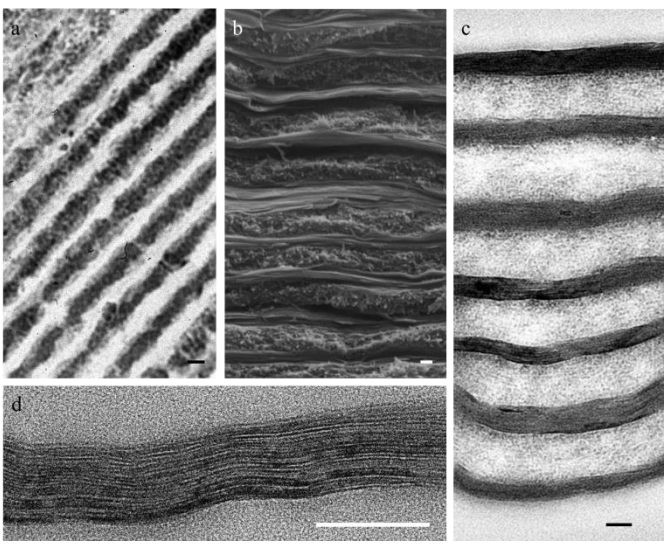

Fig. 2 (a) TEM cross-section image of the elytra of a *C. rajah* beetle. (b) SEM cross-section image of the $(AB)_{24}A$ film. TEM cross-section images of the (c) entire $(AB)_6A$ film and (d) a single A layer. Scale bars in all images represent 100 nm.

C. rajah beetle's elytra exhibits a green appearance with a slight blue reflection at the edge, where the surface curvature gives rise to a greater incidence angle (Fig. 3a).[4] The fabricated Bragg stacks appear green to the human eye, as shown in Fig. 3b. The stacks were prepared with varying $(AB)_nA$ combinations. Each stack combination is separated by a tide mark that runs horizontally across the film. The tide marks are created by the small differences in height between solutions into which they have been dipped. Lower color reflectance around the edges of the film is a result of water run off during the washing and drying process. Air blown onto the film pushes the water outwards and downwards, thereby increasing the area of lower color reflectance down the film. Unlike the *C. rajah* elytra, the LbL-assembled film is flat, so iridescence is not discernable until it is tilted. The relatively even green color across a large part of the surface area is a result of the consistency in the layer thicknesses that make up the stack and produce a relatively narrow reflection band (Fig. 3c). If the layer thicknesses varied during fabrication, a broader reflection band would result and appear more optically saturated to the observer.[44]

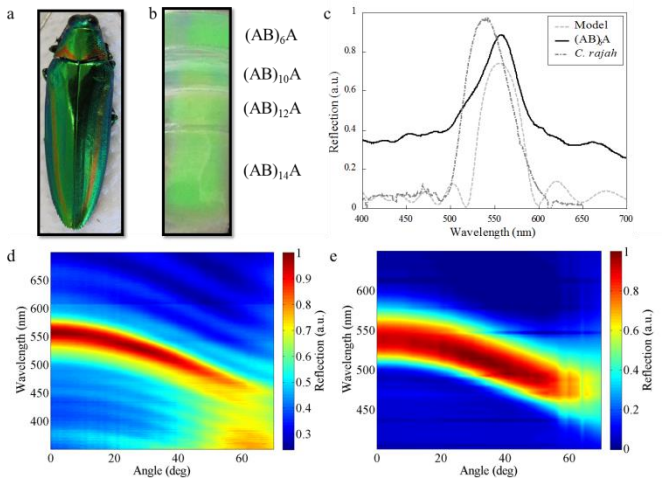

Fig. 3 Photographs of the (a) *C. rajah* beetle and (b) LbL-assembled Bragg stacks showing 4 different stacks with 13 $[(AB)_6A]$, 21 $[(AB)_{10}A]$, 25 $[(AB)_{12}A]$ and 29 $[(AB)_{14}A]$ layers (or stripes) of varying RI. (c) Reflection spectra taken from a green region of a *C. rajah* elytron and the fabricated $(AB)_6A$ stack. Color plots showing reflection as a function of wavelength and incidence angle for the (d) $(AB)_6A$ film and (e) *C. rajah* beetle.

The data set in Fig. 3c shows reflection curves for both the *C. rajah* beetle and the LbL-assembled Bragg stack (this stack is representative of all stacks $(AB)_{10\text{-}24}A$) and the modelled data. Fig. 3d and e show normalized dispersion plots of reflection as a function of wavelength and angle of incidence. Discernable in each plot is the blue-shift of the peak reflection with an increasing incidence angle. This behavior is indicative of the iridescent optical behaviour of each system. The shift is stronger in the fabricated Bragg stack, with its peak reflected wavelength shifting ~110 nm (compared to ~70 nm for the *C. rajah* for the same change in angle). The iridescence of the LbL-assembled Bragg stack is comparable to multilayer films produced by magnetron sputtering[45] and stronger than films with incorporated microlenses.[46]

Conclusions

Thin, multilayered, structurally-colored films incorporating polyelectrolyte/clay and colloidal silica/cellulose nanocrystals layers were prepared by LbL deposition. This multilayered stack was tuned to exhibit similar optical properties to that of the integument of the *C. rajah* beetle. Layer composition produced the appropriate refractive indices and layer thicknesses were controlled by the number of LbL deposition cycles. The structure within the films comprises alternating low and high RI layers with thicknesses on the order of visible light. The fabricated film appears green, possessing a narrow reflectance band matching both the optical model and the *C. rajah* beetle. As expected, the film is also iridescent since the reflected wavelength blue-shifts with increasing incidence angle. This water-based deposition technique is simple and can be scaled up to a low cost continuous process.

Acknowledgements

SJE and JCG thank the Royal Society International Exchanges Programme (IE130735) and PV the USAF (FA9550-10-1-0020) for their financial support of this work. JCG and PT also acknowledge the Texas A&M Engineering Experiment Station for infrastructural support and the National Science Foundation (CBET 1403686) for financial support of this work.

References

1. M. Srinivasarao, *Chem. Rev.*, 1999, **99**, 1935-1961.
2. C. W. Mason, *J. Phys. Chem.*, 1926, **30**, 383-395.
3. P. Vukusic and J. R. Sambles, *Nature*, 2003, **424**, 852-855.
4. J. A. Noyes, P. Vukusic and I. R. Hooper, *Opt. Express*, 2007, **15**, 4351-4358.
5. A. E. Seago, P. Brady, J. P. Vigneron and T. D. Schultz, *J. Roy. Soc. Interface*, 2009, **6**, S165-S184.
6. J. P. F. Lagerwall, C. Schutz, M. Salajkova, J. Noh, J. H. Park, G. Scalia and L. Bergstrom, *Npg Asia Mater.*, 2014, **6**.
7. M. F. Land, *Prog. Biophys. Mol. Biol.*, 1972, **24**, 75-106.
8. M. A. Haque, T. Kurokawa and J. P. Gong, *Soft Matter*, 2012, **8**, 8008-8016.
9. M. N. Ghazzal, O. Deparis, A. Errachid, H. Kebaili, P. Simonis, P. Eloy, J. P. Vigneron, J. De Coninck and E. M. Gaigneaux, *J. Mater. Chem.*, 2012, **22**, 25302-25310.
10. P. Kurt, D. Banerjee, R. E. Cohen and M. F. Rubner, *J. Mater. Chem.*, 2009, **19**, 8920-8927.
11. M. Kreysing, R. Pusch, D. Haverkate, M. Landsberger, J. Engelmann, J. Ruiter, C. Mora-Ferrer, E. Ulbricht, J. Grosche, K. Franze, S. Streif, S. Schumacher, F. Makarov, J. Kacza, J. Guck, H. Wolburg, J. K. Bowmaker, G. von der Emde, S. Schuster, H. J. Wagner, A. Reichenbach and M. Francke, *Science*, 2012, **336**, 1700-1703.
12. N. S. Allen, M. Edge, A. Ortega, C. M. Liauw, J. Stratton and R. B. McIntyre, *Polym. Degrad. Stabil.*, 2002, **78**, 467-478.
13. H. Lachheb, E. Puzenat, A. Houas, M. Ksibi, E. Elaloui, C. Guillard and J. M. Herrmann, *Appl. Catal. B-Environ.*, 2002, **39**, 75-90.
14. P. Amezaga-Madrid, W. Antunez-Flores, I. Monarrez-Garcia, J. Gonzalez-Hernandez, R. Martinez-Sanchez and

M. Miki-Yoshida, *Thin Solid Films*, 2008, **516**, 8282-8288.
15. H. Randhawa, *Thin Solid Films*, 1991, **196**, 329-349.
16. R. Robles, N. Barreau, A. Vega, S. Marsillac, J. C. Bernede and A. Mokrani, *Opt. Mater.*, 2005, **27**, 647-653.
17. W. D. Sproul, *J. Vac. Sci. Technol. A*, 1994, **12**, 1595-1601.
18. M. N. Ghazzal, O. Deparis, J. De Coninck and E. M. Gaigneaux, *J. Mater. Chem. C*, 2013, **1**, 6202-6209.
19. M. Barhoum, J. M. Morrill, D. Riassetto and M. H. Bartl, *Chem. Mater.*, 2011, **23**, 5177-5184.
20. G. M. Nogueira, D. Banerjee, R. E. Cohen and M. F. Rubner, *Langmuir*, 2011, **27**, 7860-7867.
21. O. Svensson, L. Lindh, M. Cardenas and T. Arnebrant, *J. Colloid Interf. Sci.*, 2006, **299**, 608-616.
22. M. A. Priolo, K. M. Holder, D. Gamboa and J. C. Grunlan, *Langmuir*, 2011, **27**, 12106-12114.
23. S. S. Shiratori and M. F. Rubner, *Macromolecules*, 2000, **33**, 4213-4219.
24. J. Irigoyen, L. Han, I. Llarena, Z. W. Mao, C. Y. Gao and S. E. Moya, *Macromol. Rapid Comm.*, 2012, **33**, 1964-1969.
25. H. L. Tan, M. J. McMurdo, G. Pan and P. G. Van Patten, *Langmuir*, 2003, **19**, 9311-9314.
26. J. S. Shi, F. Hua, T. H. Cui and Y. M. Lvov, *Chem. Lett.*, 2003, **32**, 316-317.
27. H. Y. Zhang, D. Wang, Z. Q. Wang and X. Zhang, *Eur. Polym. J.*, 2007, **43**, 2784-2791.
28. J. E. Wong, A. M. Diez-Pascual and W. Richtering, *Macromolecules*, 2009, **42**, 1229-1238.
29. P. Podsiadlo, M. Michel, J. Lee, E. Verploegen, N. W. S. Kam, V. Ball, Y. Qi, A. J. Hart, P. T. Hammond and N. A. Kotov, *Nano Lett.*, 2008, **8**, 1762-1770.
30. D. A. Hagen, B. Foster, B. Stevens and J. C. Grunlan, *ACS Macro Lett.*, 2014, **3**, 663-666.
31. M. Alba, P. Formentin, J. Ferre-Borrull, J. Pallares and L. F. Marsal, *Nanoscale Res. Lett.*, 2014, **9**.
32. E. C. Dreaden, S. W. Morton, K. E. Shopsowitz, J. H. Choi, Z. J. Deng, N. J. Cho and P. T. Hammond, *ACS Nano*, 2014, **8**, 8374-8382.
33. M. A. Priolo, D. Gamboa, K. M. Holder and J. C. Grunlan, *Nano Lett.*, 2010, **10**, 4970-4974.
34. D. Kim, P. Tzeng, K. J. Barnett, Y. H. Yang, B. A. Wilhite and J. C. Grunlan, *Adv. Mater.*, 2014, **26**, 746-751.
35. K. V. Gobi and F. Mizutani, *Sensor. Actuat. B-Chem.*, 2001, **80**, 272-277.
36. P. P. Campos, M. L. Moraes, D. Volpati, P. B. Miranda, O. N. Oliveira and M. Ferreira, *ACS Appl. Mater. Interfaces*, 2014, **6**, 11657-11664.
37. S. Sunny, N. Vogel, C. Howell, T. L. Vu and J. Aizenberg, *Adv. Funct. Mater.*, 2014, **24**, 6658-6667.
38. X. Du, X. Y. Li and J. H. He, *ACS Appl. Mater. Interfaces*, 2010, **2**, 2365-2372.
39. D. Patra, P. Vangal, A. A. Cain, C. Cho, O. Regev and J. C. Grunlan, *ACS Appl. Mater. Interfaces*, 2014, **6**, 16903-16908.
40. A. A. Cain, M. G. B. Plummer, S. E. Murray, L. Bolling, O. Regev and J. C. Grunlan, *J. Mater. Chem. A*, 2014, **2**, 17609-17617.
41. A. J. Mateos, A. A. Cain and J. C. Grunlan, *Ind. Eng. Chem. Res.*, 2014, **53**, 6409-6416.
42. K. C. Krogman, R. E. Cohen, P. T. Hammond, M. F. Rubner and B. N. Wang, *Bioinspir. Biomim.*, 2013, **8**.
43. P. Podsiadlo, L. Sui, Y. Elkasabi, P. Burgardt, J. Lee, A. Miryala, W. Kusumaatmaja, M. R. Carman, M. Shtein, J. Kieffer, J. Lahann and N. A. Kotov, *Langmuir*, 2007, **23**, 7901-7906.
44. T. Alfrey, E. F. Gurnee and W. J. Schrenk, *Polym. Eng. Sci.*, 1969, **9**, 400-&.
45. O. Deparis, M. Rassart, C. Vandenbem, V. Welch, J. P. Vigneron, L. Dreesen and S. Lucas, *Plasma Process. Polym.*, 2009, **6**, S746-S750.
46. T. Scharf, S. Jaquet, P. Ruffieux and H. P. Herzig, *Jpn. J. Appl. Phys.*, 2008, **47**, 6699-6705.

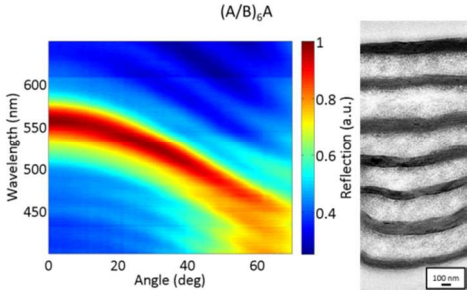

The Layer-by-Layer fabricated systems exhibited similar optical behavior to the Coleoptera beetle, reflecting the desired color and displaying iridescent behavior.